4 Similarity Theory

4.1 Motivation

In the statistical description of turbulence we have seen that the turbulence can, under certain circumstances, be separated from the mean flow and, formally, be introduced through Reynolds decomposition and averaging. Also, it was noted that products of variables under this treatment do lead to 'new variables', i.e. the co-variances ($\overline{a'b'}$ - cf. Table 3.1)[1], which were identified to sometimes even dominate the characteristics of the flow. When formally applying 'Reynolds decomposition and averaging' to the set of the conservation equations for atmospheric flows (as will be done in Chapter 5) we will find that a fundamental problem arises from this approach: the more equations we treat in this manner the more unknowns ('new variables') we are faced with. And the more conservation equations we derive for these unknowns, the more additional unknowns enter the problem. This is the so-called *closure problem*. Still, this approach is instrumental for the construction of numerical models and solutions (closure assumptions) will be introduced in Section 5.2.

However, a fundamentally different approach can be taken that does not seek to find a (analytical or numerical) solution to this problem. Rather, this approach attempts to find out whether there are means to predict the 'characteristics of the result'. Thus this approach employs the following arguments:

- A turbulent flow *could* in fact be treated by traditional methods of fluid mechanics. However then, resolved time and space scales would have to be on the order of seconds and millimetres, respectively (see Chapter 7, spectral characteristics).
- Thus, Reynolds decomposition and averaging *is* invoked, thereby employing the *spectral gap*, which conveniently separates the scales of mean flow and turbulence (Chapter 3).
- The newly introduced co-variances are identified with important physical processes, i.e. turbulent transport of momentum, sensible and latent heat and it is *observed* that these new variables under certain circumstances even dominate the problem[2].
- An independent theory is then sought to describe these new variables independently from the conservation equations. *Similarity theory* is such an approach.

Note that for some problems the formal approach is more promising and for other problems it is similarity theory. The majority of problems will even

[1] In Chapter 5 we will see that also higher order moments will eventually enter the problem.

[2] In terms of a formal scale analysis, this means that the terms including these turbulent fluxes dominate the respective conservation equation.

require elements of both. Prominent examples for the latter are numerical models: the formal approach is adopted in order to derive a basic form of the conservation equations that are solved in finite-difference form on a grid. For the scales between grid resolution and the smallest turbulence scales then, similarity arguments are employed (as a so-called turbulence closure assumption, see Chapter 6).

4.2 Scaling and Similarity

Often, unqualified statements like 'a kilogram of rice costs only 5 cents in this or that developing country' can be heard. By changing this into the more informative 'a kilogram of rice costs a farmer in that country 5% of his average weekly salary', the result has been *scaled*, in this case with the weekly salary. Another example for the usefulness of scaling may be the case when an unknown variable can more easily be estimated from its ratio to another quantity. Consider the (unlikely) task to estimate the head diameter of a large number of human beings – all Europeans, say. Rather than measuring all the heads a fruitful approach may consist in establishing, on the basis of a smaller sample, the average ratio between head diameter and height of a person. This may well even turn out to be roughly constant. Then the head diameter can easily be estimated from the information available in every passport.

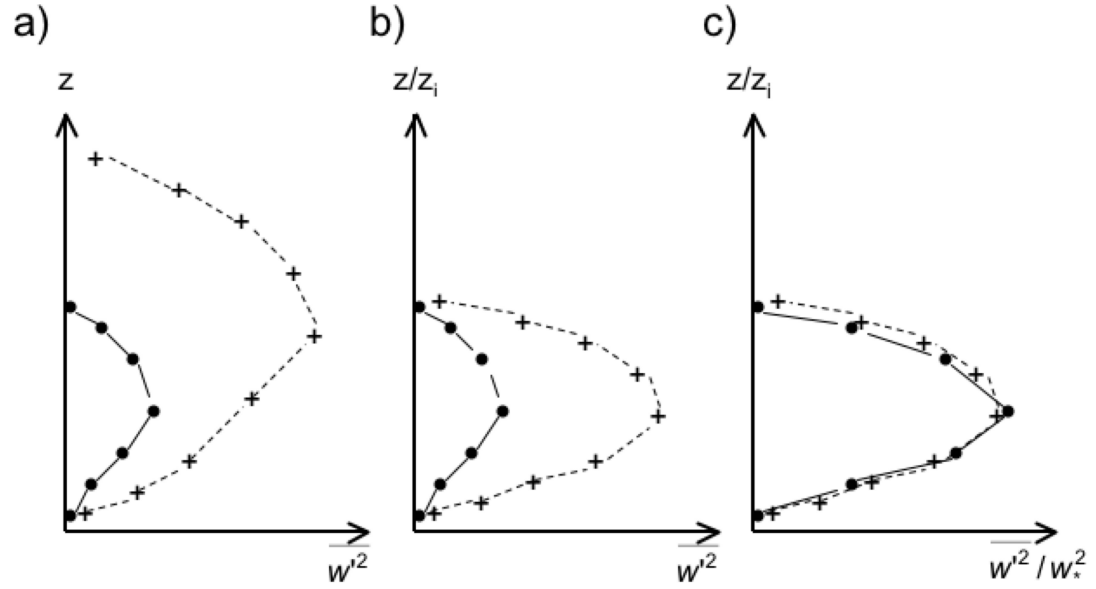

Figure 4.1 a) Two hypothetical observations of the vertical velocity variance in a CBL; b) as in a) but with scaled height axis, and c) with both axes scaled.

Another issue, although related of course, is *similarity*. Figure 4.1a shows two observations of the vertical velocity variance. Apparently the two curves are similar, even if at a certain height one reading is at maximum while the other already vanishes. Noting that the height where the turbulence vanishes might be identified with the 'mixed layer height' yields Fig. 4.1b where the vertical axis is scaled with z_i (mixed layer height). Choosing the 'right' scaling variable

also for the velocity variance (denoted w_*^2 here for convenience), finally, leads to Fig. 4.1c. If correspondingly good results are obtained for a large number of cases, this means that under the given conditions (unstable boundary layer, in the example) the chosen characteristic velocity (w_* - and hence the variables from which it is formed: see below) characterises the magnitude of the vertical velocity variance as a function of relative height within the CBL.

The remainder of this chapter deals with objective methods to find the appropriate scaling variables and with the presentation of some so-called *scaling regimes*.

4.3 Practical Approach

Similarity theory as it is usually employed in boundary layer meteorology is based on a four-step procedure that is outlined below using the terminology of Stull (1988). These four steps are:

1 Determine the *relevant processes* (or the corresponding characteristic variables) that determine the phenomenon to be described.

2 Determine the maximum number N of independent non-dimensional so-called π*-groups* by using Buckingham's π*-Theorem.*

3 Any[3] other mean variable of interest, $\overline{a}$, that is made dimensionless by appropriate scaling variable (a_*) may then be expressed as

$$\frac{\overline{a}}{a_*} = f_a(\pi_1, \pi_2, ...\pi_N) \qquad (4.1)$$

4 Finally, make *an experiment* to determine f_a. It is important to notice that similarity theory as such does not make any prediction on the shape of this function, but clearly other knowledge may be used to specify certain conditions (e.g., limiting values, etc.)

1) Relevant processes

This is indeed the most important (and also most difficult) step in the procedure. Only the result (step 4) will tell whether or not the right process choices have been made. In the example of Fig. 4.1 the choice was apparently successful[4]. If an important process is not considered, the result will show large scatter. On the other hand, if too many processes are identified as important, one (or more) π*-groups* will drop out as irrelevant.

2) Buckingham's π-Theorem

[3] In principle, all variables that respond to the same processes (as defined in step 1) will follow the assertion of step 3. In practice, exceptions may exist thus indicating that for this particular variable the chosen processes are not sufficient.

[4] The example is constructed, but it follows experience from *Mixed Layer Scaling* (see Section 4.5)

This theorem states that in a system with

n Variables

r fundamental physical dimensions (*m, kg, s, K, Ampere)*

there are exactly $N = n - r$ possible independent dimensionless π*-groups.* Following Stull (1988) a practical approach ('recipe') for the application of this theorem can be given as follows.

A) Let the problem have *n* variables and *r* physical dimensions.

B) *Choose* among the *n* variables *r key variables* under the condition that

→ all fundamental dimensions are represented

→ no dimensionless combination of the key variables must be possible

C) Determine the 'dimensions-equations' for the remaining (not key) variables.

D) Solve the 'dimensions-equations' to determine the exponents.

E) For each of these equations: divide the lhs by the rhs (or vice versa) to obtain the π*-groups.*

To illustrate this procedure it will be demonstrated by a few examples in this and the next section.

3) Scaling variables

The scaling variables are chosen from the pool of *n* variables and are also determined by solving the 'dimensions-equations'. Clearly, a scaling variable must have the same physical dimensions as the variable to be scaled.

4) Experiment

As stated above, the experiment will yield the shape of function f_a in (4.1) and will also indicate whether our choice of processes (variables) had been appropriate. If the scatter is *sufficiently small* we can be sure to have made the right choices. It is clear that in an environmental system (as the atmospheric boundary layer) we will rarely obtain 'no scatter at all' - even if the relevant (and not too many) processes are included. Still, in most cases it is quite obvious whether the result just reflects natural variability and observational uncertainty or indeed a bad choice of variables.

Before turning our attention to scaling in the ABL it might be instructive to consider an example that is very familiar to atmospheric scientists (and is usually obtained by quite different means): the *Geostrophic wind*. In describing the wind field on the synoptic scale we have essentially four variables, which determine the flow: the air density (ρ in $[kgm^{-3}]$), the Coriolis parameter (f in $[s^{-1}]$), a Length scale (L_* in $[m]$) and the pressure difference (Δp in $[kgs^{-2}m^{-1}]$) with $r = 3$ physical dimensions. Thus we have only $N = 1$ π *-group*. Let us choose f, L_* and Δp as key variables. It is easily verified that no non-trivial dimensionless combination of the three is possible since the

mass appears in only one of them. The dimension's equation for the last variable reads

$$\rho = (\Delta p)^a \cdot (L_*)^b \cdot (f)^c \tag{4.2}$$

Thus the three equations for the physical dimensions read

$$\begin{aligned} kg: &\quad 1 = a \\ m: &\quad -3 = -a + b \\ s: &\quad 0 = -2a \quad \text{- c} \end{aligned} \tag{4.3}$$

with the ready solution a=1, b=-2, c=-2. The density can therefore be expressed as

$$\rho = \frac{\Delta p}{L_*^2 f^2} \tag{4.4}$$

and the single π*-group* is

$$\pi_1 = \frac{\rho L_*^2 f^2}{\Delta p} \tag{4.5}$$

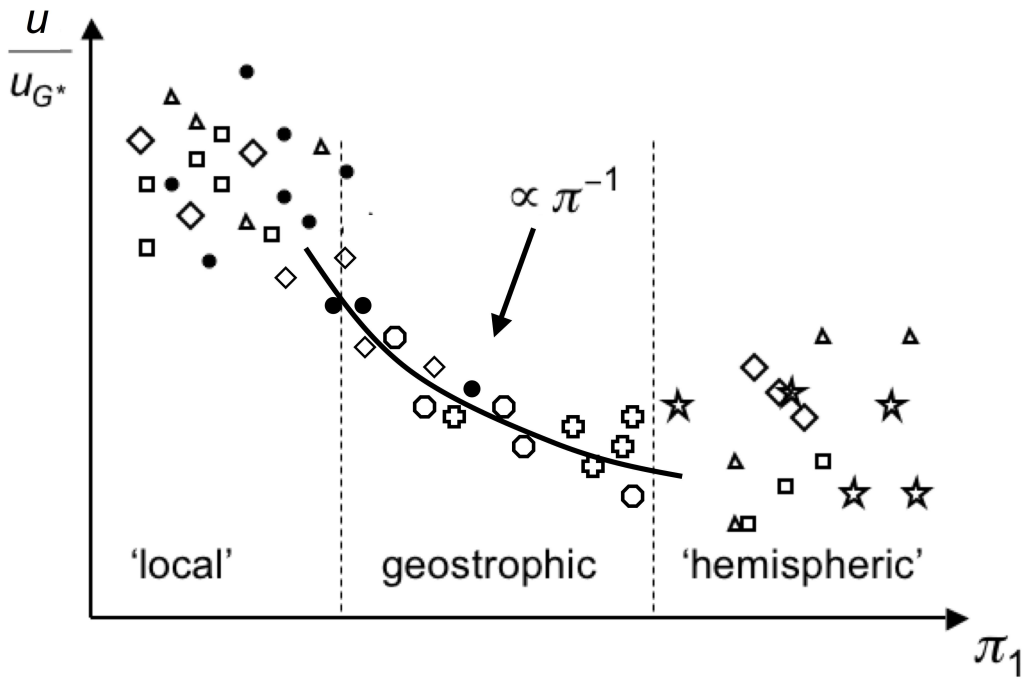

Figure 4.2 Hypothetical data for the similarity prediction of the Geostrophic wind. Different symbols may denote 'data' from different platforms, experiments, seasons, etc.

As our variable of interest is the (Geostrophic) wind speed, u_G, we try to find a scaling variable, u_{G*}. The easiest choice from the pool of available variables is $u_{G*} = L_* f$ with the desired dimensions [ms^{-1}]. Equation (4.1) then predicts that

$$\frac{u_G}{u_{G^*}} = f_G(\pi_1), \text{ or } \quad u_G \propto fL_* \cdot f_G(\pi_1) \tag{4.6}$$

Using atmospheric data ('experiment') and plotting them according to the above similarity prediction we will then find that $f_G(\pi_1) \propto \pi^{-1}$ (see Fig. 4.2). In other words the similarity prediction for wind speed for a certain range of π_1 (to be identified with the synoptic scale) would be

$$u_G \propto \frac{1}{\rho f}\frac{\Delta p}{L_*}, \tag{4.7}$$

and this corresponds to the familiar result we usually obtain from scale analysis for the conservation equations of momentum. Figure 4.2 also shows how the result may look like for too small π_1 (or too small L_*), i.e. for local flows and too large π_1 (hemispheric scales).

According to Eq. (4.1) *any mean variable* $\bar{a}$ of the 'system' under consideration, if appropriately scaled, can be described through *a universal function* f_a. Therefore, if the 'system' is a particular locus within the PBL (for example the layer near the surface under conditions of stable stratification) the characteristics of this variable are known anywhere in the world and at any time - if only the shape of this function is known and its arguments can be determined. In Section 4.5 the most important loci ('scaling regimes') will be described in some detail.

4.4 Monin-Obukhov Similarity Theory for the Surface Layer

The probably best and most extensively treated example for the similarity approach is Monin and Obukhov's (1954) theory for the Surface Layer. We discuss its properties in some detail in the following.

In the Surface Layer (SL) friction plays an important role, as well as surface exchange of sensible heat. We may therefore choose $\overline{u'w'}_o$ and $\overline{w'\theta'}_o$, the surface fluxes of momentum and sensible heat as relevant variables. In this context it is important to note that the *surface* values are chosen because the turbulent transport in this case has its origin at the surface and is therefore at maximum there. At the same time the turbulent fluxes do not significantly vary with height[5] within the SL (less that 10%, and this roughly corresponds to a good accuracy they can experimentally be determined) so that indeed the surface values are *characteristic* for the SL. As an additional process buoyancy must be considered through the buoyancy parameter ($g/\bar{\theta}$). Finally as a length scale we use the height z. From these four variables with three physical dimensions Buckingham's Theorem predicts $N = 4 - 3 = 1$ independent π*-group*. Let us then choose $\overline{u'w'}_o$, $\overline{w'\theta'}_o$ and $g/\bar{\theta}$ as key

[5] The SL is therefore sometimes referred to as the *constant flux layer*. In practice this fact also allows one to determine the fluxes at any height within the SL and interpret them as surface fluxes.

variables. Dimensional analysis will tell us whether this is an appropriate choice: If indeed a dimensionless combination of the three key variables were possible the dimension's equation would read

$$[0,0,0] = (\overline{u'w'_o})^a \cdot (\overline{w'\theta'_o})^b \cdot (\frac{g}{\overline{\theta}})^c . \tag{4.8}$$

Solving the three resulting equations for [*m*], [*s*], and [*K*] then yields e only solution $a = b = c = 0$, thus showing that indeed no dimensionless combination is possible. Step 'C' in the 'recipe' for the Buckingham Theorem then reads

$$z = (\overline{u'w'_o})^a \cdot (\overline{w'\theta'_o})^b \cdot (\frac{g}{\overline{\theta}})^c \tag{4.9}$$

and the solution is easily obtained

$$z = \frac{(\overline{u'w'_o})^{3/2}}{\frac{g}{\overline{\theta}}\overline{w'\theta'_o}}, \text{ or } \pi_1 = \frac{z\frac{g}{\overline{\theta}}\overline{w'\theta'_o}}{(\overline{u'w'_o})^{3/2}} \tag{4.10}$$

This is essentially the scaling result for the SL and every scaled mean variable in the SL should be expressible as a function of π_1 alone.

However, Monin and Obukhov (1954) took a slightly different approach in their original derivation by defining *characteristic variables* before starting the dimensional analysis. For friction they used the friction velocity (3.24) and *defined* a characteristic temperature scale to take into account surface heat exchange

$$\theta_* \equiv -\overline{w'\theta'_o} / u_* \tag{4.11}$$

Then a length scale, L, was introduced[6] according to

$$L \equiv \frac{1}{k}\frac{u_*^2}{\theta_*}(\frac{g}{\overline{\theta}})^{-1} = -\frac{1}{k}\frac{u_*^3}{\overline{w'\theta'_o}}(\frac{g}{\overline{\theta}})^{-1} \tag{4.12}$$

With this, the dimensionless group is z/L. Comparing (4.12) with (4.10) readily shows that the only difference in these two formulations (except for the sign, which only changes the sign of involved experimental parameters) is that the Obukhov length, L, includes the v. Kàrmàn constant[7], $k \approx 0.4$. From its definition the Obukhov length has a pole when approaching neutral conditions ($\overline{w'\theta'_o} \to 0$) and thus $|z/L| \to 0$. For convective conditions the surface heat flux is positive and hence $z/L < 0$ and for stable conditions the opposite is true.

---

[6] In fact this length scale was already employed in a paper by Obukhov (1946) and will be referred to as Obukhov Length.

[7] This constant was taken into account to ensure that the new theory of Monin and Obukhov (which for the first time included thermal turbulence) was compatible with the 'standard theory' in those days, valid only for *neutral* flows.

Finally, in the SL according to Monin-Obukhov similarity theory (4.1) reads

$$\frac{\bar{a}}{a_*} = f_a(z/L) \qquad (4.13)$$

In other words, any dimensionless mean variable is predicted to be a function of z/L alone. Figure 4.3 shows that this prediction is sometimes extremely good, as that for the mean non-dimensional gradient for wind speed during the famous 'Kansas experiment' in the early 1970ies. For other variables, or when combining data from different experiments the scatter may be somewhat more important.

Two aspects require explicit mentioning when discussing Monin-Obukhov Similarity Theory (MOST). The non-dimensional groups in (4.10) and (4.12) are only equal if $\overline{v'w'_o} = 0$ (cf. the definition of the friction velocity, 3.24). If the coordinate system is rotated into the mean flow direction and if the assumption of horizontally homogeneous conditions holds, indeed the directional shear ($\overline{v'w'_o}$) vanishes and only frictional shear can be used in the definition of the friction velocity. Under most practical conditions, however, it is advisable to use the full definition for the friction velocity. Second, so far we have considered a dry boundary layer. If we are interested in water vapour we may extend the similarity analysis by taking into account an additional relevant process (evaporation) and hence an additional variable (usually taking the kinematic latent heat flux at the surface $\overline{w'q'}_o$, where q' is the water vapour mixing ratio. This then defines a characteristic humidity scale according to $q_* = -\overline{w'q'}/u_*$). This adds an additional variable, but also an additional physical unit (kg[8]) to the problem, so that according to the approach as outlined in Section 4.3 we have $N = n - r = 5 - 4 = 1$ and hence one non-dimensional group (z/L) determines the turbulences state in the SL.

4.5 Scaling Regimes

In an important paper Holtslag and Nieuwstadt (1986) summarised the scaling regimes for the idealised (i.e., horizontally homogeneous and quasi-stationary) ABL. Figure 4.4 shows their non-dimensional representation of the unstable (Fig. 4.4a) and stable (Fig. 4.4b) ABL. The regimes are represented as a function of non-dimensional height (z/h), where h denotes both the mixed layer height[9] and the height of the stable boundary layer and non-dimensional stability h/L, where L is the Obukhov length (4.12). All scaling regimes are identified with their names and the relevant scaling parameters. Note that in order to follow the practical procedure as outlined in Section 4.3

[8] Even if the mixing ratio if formally dimensionless, it measures kg of water vapor relative to kg of air, thus mass formally enters the problem).

[9] Standard notation for the ML height is z_i.

to find the non-dimensional π-groups, the buoyancy parameter $g/\overline{\theta}$ must be added to all the scaling regimes.

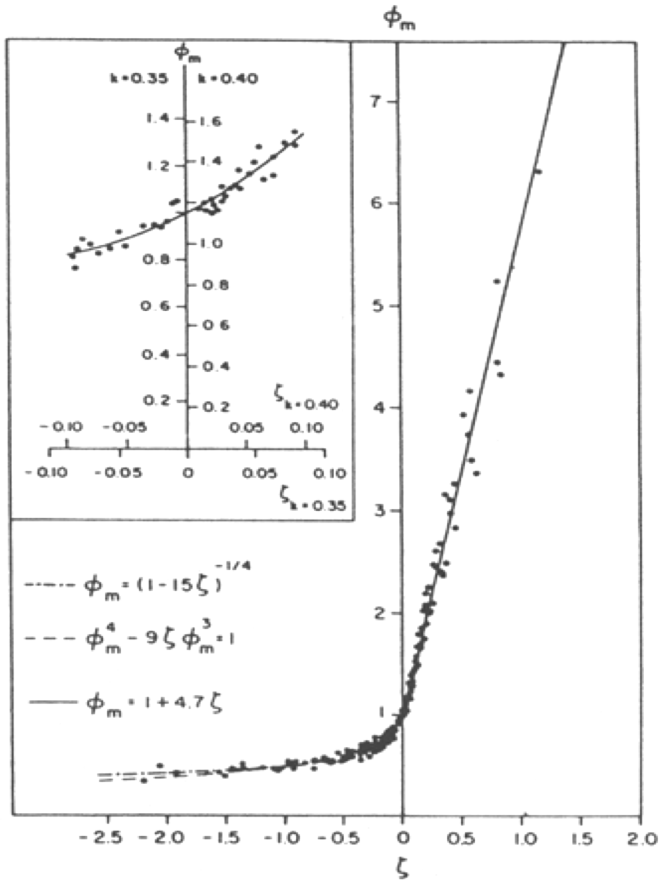

Figure 4.3 Non-dimensional wind shear after Businger et al. (1971). The variable $\zeta = z/L$ is just introduced for convenience.

The 'successful' scaling regimes are those for which indeed scaling parameters are given in Fig. 4.4. This means, in the light of our discussion on quasi-stationarity (Section 3.1), that sometimes or often in such a height-stability cross-section of the ABL the forcing time scale is much larger than the time scale that describes the change of mean profiles. In this sense this finding only reflects the fact that a 'stationary description' using scaling arguments can only be successful if such conditions are predominant (or at least often exist). In the following we discuss the most important scaling regimes in some detail.

4.5.1 Surface Layer Scaling (MOST)

Over almost the entire range of stability a surface layer (SL) is indicated in the lowest 10% of the ABL in Fig. 4.4. Monin-Obukhov similarity theory for the SL has been introduced as an example for scaling in Section 4.4. Based on

(4.13), i.e. the general similarity for the SL, $\bar{a}/a_* = f_a(z/L)$, the non-dimensional profile for mean wind speed[10] in the SL is expressed as

$$\frac{\partial \bar{u}}{\partial z}\frac{kz}{u_*} = \phi_m(z/L). \tag{4.14}$$

For ideally neutral conditions ($z/L = 0$) and noting that $\phi_m(0) = 1$ can be chosen (in fact, *is chosen* by introducing the von Karman constant *k*), (4.14) can easily be integrated by separating the variables

$$\bar{u}(z_2) - \bar{u}(z_1) = \int_{u_1}^{u_2} d\bar{u} = \frac{u_*}{k}\int_{z_1}^{z_2}\frac{dz}{z} = \frac{u_*}{k}\ln(\frac{z_2}{z_1}). \tag{4.15}$$

By defining a height at which the mean wind speed vanishes, i.e., $\bar{u}(z = z_o) \equiv 0$, as the so-called *roughness length*, (4.15) yields the logarithmic wind profile for the neutral SL

$$\bar{u}(z) = \frac{u_*}{k}\ln(\frac{z}{z_o}). \tag{4.16}$$

Indeed the roughness length is not only an elegant way to express (4.15) but also characterises the underlying surface. For very smooth surfaces (e.g., fresh snow, sand or still water) it is on the order of $10^{-3}m$, for short grass or gravel some $10^{-2}m$. With increasing size of the roughness elements, also z_o increases and may be estimated at some 10% of the roughness element's height (see more detailed discussion in Chapter 10). An example for this logarithmic wind profile is given in Fig. 1.4.

Using the roughness length at the lower boundary, we can integrate (4.14) by substituting $z/L = \zeta$

$$\frac{k}{u_*}\int_0^{\bar{u}} d\bar{u}' = \int_{z_o}^{z}\frac{\phi_M(\zeta)}{z'}dz' \ . \tag{4.17}$$

While the integration of the lhs is straight forward a transformation of the rhs is performed that will become clear below:

$$\frac{k}{u_*}\bar{u}(z) = \int_{z_o}^{z}\frac{dz'}{z'} - \int_{z_o}^{z}\frac{1-\phi_M(\zeta)}{z'}dz' = \ln\left(\frac{z}{z_o}\right) - \int_{z_o}^{z}\frac{1-\phi_M(\zeta)}{z'}dz' . \tag{4.18}$$

---

[10] Note that intuitively, one would possibly seek $\bar{u}/u_* = f_U(z/L)$ to obtain wind information in the SL - and a series of experiments (step 4) would yield empirical functions similar to eq. (4.16) but different for each type of surface. Thus, a length scale describing the surface would have to be introduced. Starting with the gradient, therefore, recognizes the importance of friction on flow deformation and yields a more general result (and the surface character is introduced as a boundary condition).

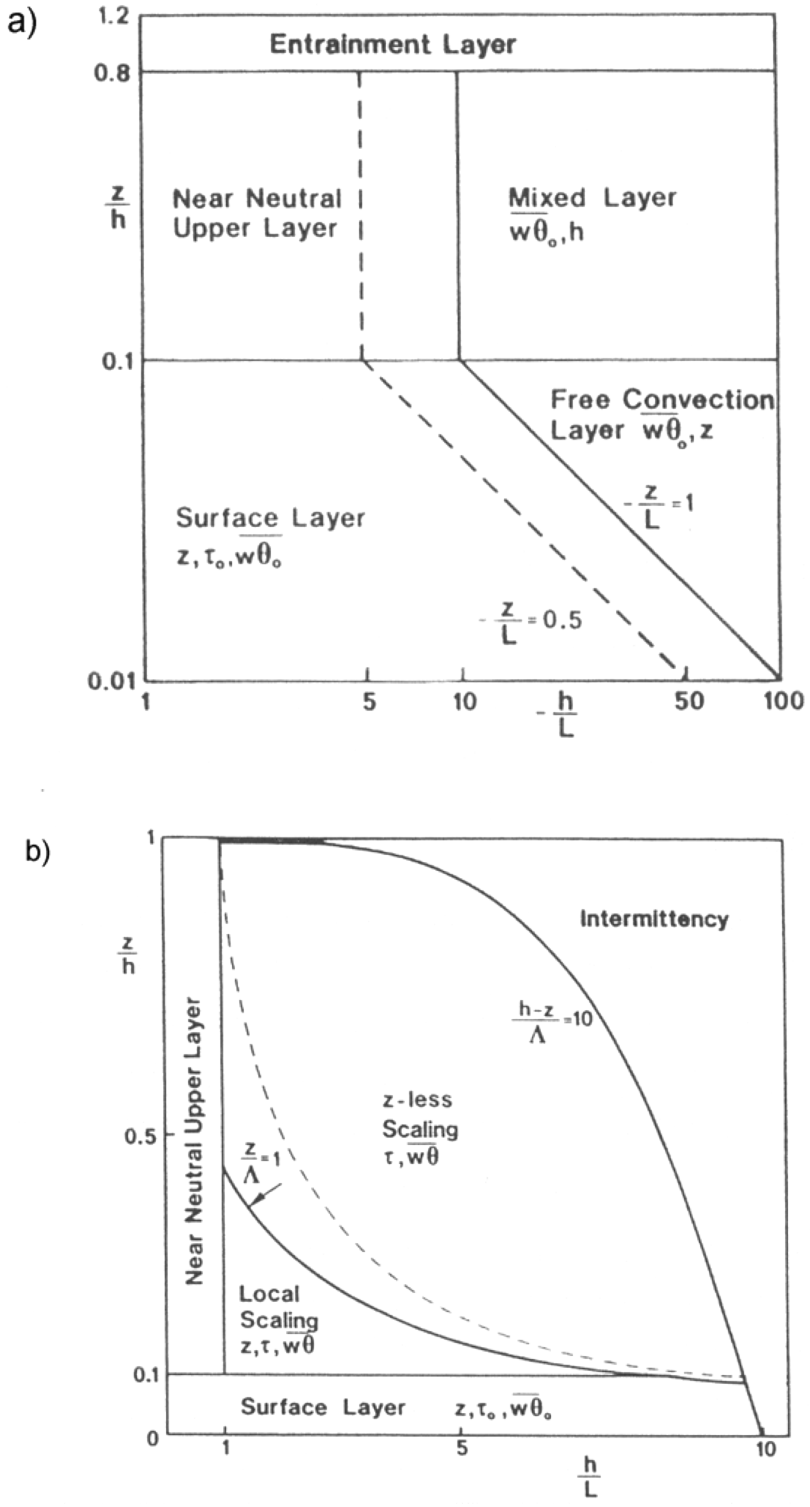

Figure 4.4a Scaling regimes for (from Holtslag and Nieuwstadt, 1986) for a) unstable and b) stable stratification. Note the different logarithmic and linear scales in Figs. 4.4a and 4.4b. *h* denotes the boundary layer height and *L* is the Obukhov length.

We now write (4.18) in terms of ζ and note that $\partial z/\partial\zeta = L$:

$$\frac{k}{u_*}\bar{u}(z) = \ln\left(\frac{z}{z_o}\right) - \int_{\zeta_o}^{\zeta}\frac{1-\phi_M(\zeta)}{L\zeta}\underbrace{\frac{\partial z}{\partial\zeta}}_{=L}d\zeta = \ln\left(\frac{z}{z_o}\right) - \underbrace{\int_{\zeta_o}^{\zeta}\frac{1-\phi_M(\zeta)}{\zeta}d\zeta}_{=:\Psi_M(\zeta)}. \qquad (4.19)$$

Equation (4.19) defines the integrated form of the non-dimensional wind shear, Ψ_m, which can be seen to correspond to the deviation from the logarithmic form under non-neutral conditions. The similarity prediction for the mean wind speed profile in the SL therefore reads

$$\bar{u}(z) = \frac{u_*}{k}\left[\ln\left(\frac{z}{z_o}\right) - \Psi_M(z/L)\right] \qquad (4.20)$$

For the non-dimensional gradient of wind shear ϕ_m, many different functions have been proposed based on experiments. Högström (1988) has compared all the different formulations and has brought them to comparable standards (e.g., by using the same value for the v. Kàrmàn constant). For the unstable side the most general approach is

$$\text{unstable:} \quad \phi_M = (1-\gamma z/L)^{\alpha}, \qquad (4.21)$$

where the exponent is often found to be -1/4 and $\gamma \approx 16$ (for details see Högström, 1988). For any formulation of the form (4.21) the integrated form can be determined from (Paulson, 1970):

$$\text{unstable:} \quad \Psi_M(\frac{z}{L}) = 2\ln\left[\frac{1+x}{2}\right] + \ln\left[\frac{1+x^2}{2}\right] - 2\tan^{-1}(x) + \frac{\pi}{2}, \qquad (4.22)$$

where $x = (1-\gamma z/L)^{-\alpha}$.

For the stable SL, the early experiments (e.g., Kansas) have yielded a linear dependence of ϕ_m on stability

$$\text{stable:} \quad \phi_M = 1+\beta z/L, \qquad (4.23)$$

and the integration (to yield Ψ_M) is straightforward. Often $\beta \approx 6$ is found to fit the data quite well. A more complicated formulation has been proposed by Beljaars and Holtslag (1991)

$$\text{stable:} \quad \phi_M = 1 + a\frac{z}{L} + b\frac{z}{L}\exp\left\{-d\frac{z}{L}\right\} - bd\frac{z}{L}(\frac{z}{L} - \frac{c}{d})\exp\left\{-d\frac{z}{L}\right\} \qquad (4.24)$$

(with $a = 1$, b = 0.667, c = 5 and d = 0.35) and shown to better correspond to field data from several sites (but see the discussion on z-less scaling below).

The non-dimensional gradients, and their integrated forms, for potential temperature and specific humidity are formulated in analogy to (4.14):

$$\frac{\partial\bar{\theta}}{\partial z}\frac{kz}{\theta^*}=\phi_H(z/L) \quad\rightarrow\quad \bar{\theta}(z)-\bar{\theta}(z_{oh})=\frac{\theta_*}{k}\left[\ln\left(\frac{z}{z_{oh}}\right)-\Psi_H\left(\frac{z}{L}\right)\right]$$
$$\frac{\partial\bar{q}}{\partial z}\frac{kz}{q^*}=\phi_q(z/L) \quad\rightarrow\quad \bar{q}(z)-\bar{q}(z_{oq})=\frac{q_*}{k}\left[\ln\left(\frac{z}{z_{oq}}\right)-\Psi_q\left(\frac{z}{L}\right)\right] \qquad (4.25)$$

Here, the characteristic variable for humidity, $q_*=-\overline{w'q'}_o/u_*$, has been introduced through the surface flux of latent heat. Note that in general the 'roughness lengths' for temperature and humidity are not equal to that for momentum and also these variables do not vanish by definition at this datum. In fact, it is very difficult to experimentally determine z_{oh} and z_{oq}. For heat, often the longwave outgoing radiation according to the law of Stefan-Boltzmann, $LW\uparrow=\varepsilon\sigma T_s^4$, is used where T_s corresponds to the 'surface' temperature, i.e. supposedly to that at z_{oh}. This, however, challenges the accuracy of radiation measurements, which is usually not good enough to determine the roughness length to within an order of magnitude (Malhi 1996; Calanca, 2001). For moisture, on the other hand it is usually assumed that the air is saturated at the surface so that z_{oq} can be determined as the height where saturation occurs (for what we again need the 'surface temperature').

Over homogeneous surfaces, z_{oh} is often found to be about an order of magnitude smaller than the roughness length for momentum (Malhi 1996, Verma 1989). There is, however, a pronounced impact of surface character ('bluff body' type roughness as for sand grains vs. 'permeable roughness' like grass or other vegetation), which is often expressed in terms of a dependence of $\ln(z_o/z_{oh})$ on the roughness Reynolds number, $\mathrm{Re}^*=z_o u_*/\upsilon$ (e.g., Verma 1989; Sun 1999). The sparse available studies suggest only small differences between the roughness lengths for heat and moisture (Verma 1989).

The standard deviation of vertical velocity is found to obey the relation

$$\text{unstable: } \frac{\sigma_w}{u_*}=1.3(1-3\frac{z}{L})^{1/3}. \qquad (4.26)$$

Under stable conditions, large scatter is usually observed (mainly due to generally weak turbulence and correspondingly large experimental uncertainty). It is often concluded that σ_w/u_* is essentially constant at approximately 1.3, i.e. does not vary with z/L. This is in line with the *local scaling* approach as discussed below.

SL formulations have also been proposed for the horizontal velocity standard deviations but the scatter is usually such that these examples might rather be used in a textbook to show how 'failure' of the prediction looks like (see Section 4.3 – step 4). Still, there is common sense that both these variables assume a characteristic value at neutrality:

Neutral: $\frac{\sigma_v}{u_*} = 1.9,\ \frac{\sigma_u}{u_*} = 2.5.$ (4.27)

The standard deviation of scalars (such as potential temperature or specific humidity), may be represented by the general relation (Sfyri et al. 2017)

$$\frac{\sigma_s}{s_*} = -a_s(b_s - c_s\frac{z}{L})^{d_s} + e_s, \quad (4.28)$$

where 's' is the scalar (such as potential temperature, $s = \theta$ or specific humidity, $s = q$). Depending on the variable and the stability range, some of the parameters can be expected to be zero or one. Others, such as d_θ for the unstable side, is expected to amount to -1/3 due to the limiting behaviour for for $z/L \to -\infty$, i.e. in free convection (e.g., Wyngaard 2010). Figure 4.5 shows scaled temperature and humidity data from the well-known reference site in Cabauw (NL) according to Sfyri et al (2017).

It should be noted that the fit to eq. (4.28) is made separately for different stability ranges on the unstable temperature data. The unstable range ($z/L < -0.05$) yields parameters close to those obtained from the 'classical' experiments (e.g., Tillmann, 1972), i.e., $a_\theta = 0.99,\ b_\theta = 0.063,\ c_\theta = 1,$ $d_\theta = -1/3,\ e_\theta = 0$). For the near-neutral range ($-0.05 < z/L < 0$), scaling with θ_* suggests that a constant 'neutral' value is approached for $z/L \to 0$ - as suggested by Tillmann, (1972) - only if the temperature variance goes to zero at the same pace as the heat flux does. Based on a simplified temperature variance budget, Tampieri et al. (2009), suggested an exponent $d_\theta \approx -1$, which fits the data well on the unstable side (Fig. 4.5, top left), while the best fit yields $d_\theta = -1.4$ for the stable temperature data (Sfyri et al. 2017).

On the stable side the scatter for the scaled temperature fluctuations is relatively large and outside the near-neutral range a constant non-dimensional temperature fluctuation seems to be approached.

Since the latent heat flux (and hence q_*) does not necessarily go to zero under neutral conditions, so that σ_q / q_* approaches a constant value (≈ 2.75).

On the stable side, the scatter is quite substantial due to generally small values (and hence large experimental uncertainty) and no dependence on z/L is observed.

We will encounter many more SL predictions especially when dealing with spectra (Chapter 7) and when discussing *departures* therefrom over complex surfaces.

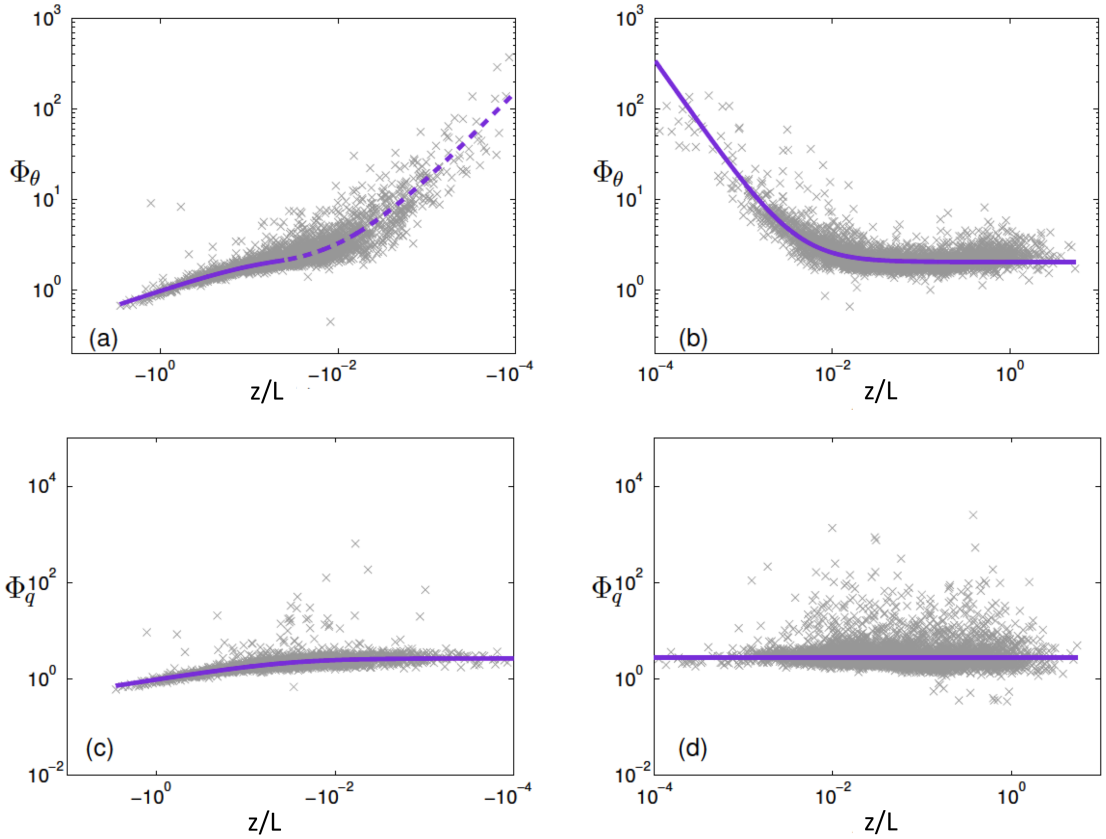

Figure 4.5 Dimensionless standard deviation of potential temperature (top row) and specific humidity (lower row) from 11 months of measurements at an almost perfectly homogeneous and flat site (in Cabauw, NL, Beljaars and Bosveld, 1997). Left column unstable and right column stable data. $\Phi_\theta = \sigma_\theta / |\theta_*|$ and $\Phi_q = \sigma_q / q_*$. Purple lines denote a fit according to eq. (4.28). For unstable temperature data (top left) the fit is performed separately for near-neutrally unstable ($-0.05 < z/L < 0$) and unstable ($z/L < -0.05$) data - with the former being shown as a dashed line. Figure slightly modified from Sfyri et al. (2017).

4.5.2 Local scaling for the SBL

Due to the suppression of turbulence under stable conditions (see Table 1.1) only small eddies are produced with a limited reach. Within the SL, still Monin-Obukhov scaling is applicable. Higher up the turbulence scales with the height z and the *local* fluxes of momentum τ_{i3} and sensible heat $\overline{w'\theta'}$ rather than with the corresponding *surface* fluxes. This is known as *Local Scaling* and has first been proposed by Nieuwstadt (1984). In effect, the local scaling (LS) approach has two elements. The first is a local Obukhov length

$$\Lambda = \frac{\tau^{3/2}}{k\frac{g}{\theta}\overline{w'\theta'}}, \qquad (4.29)$$

which is the local equivalent to (4.12) with $\tau = (\overline{u'w'}^2 + \overline{v'w'}^2)^{1/2}$ replacing u_*^2 and the local heat flux the surface heat flux. In the local scaling regime any

scaled mean variable is then expected to be dependent only on z/Λ. In other words the SL expression for scaling in the SL (4.13) becomes $\bar{a}/a_* = f_a(z/\Lambda)$ for the Local Scaling regime. Figure 4.6 shows the non-dimensional gradient of mean wind speed for a data set from a 'long-lived' SBL on the Greenland ice sheet. On the left panel SL, scaling is seen to lead to quite substantial scatter (except for the lowest measurement heights). Local scaling as displayed on the right panel is much better suited for this data set and the local equivalent of (4.24) fits the data quite well.

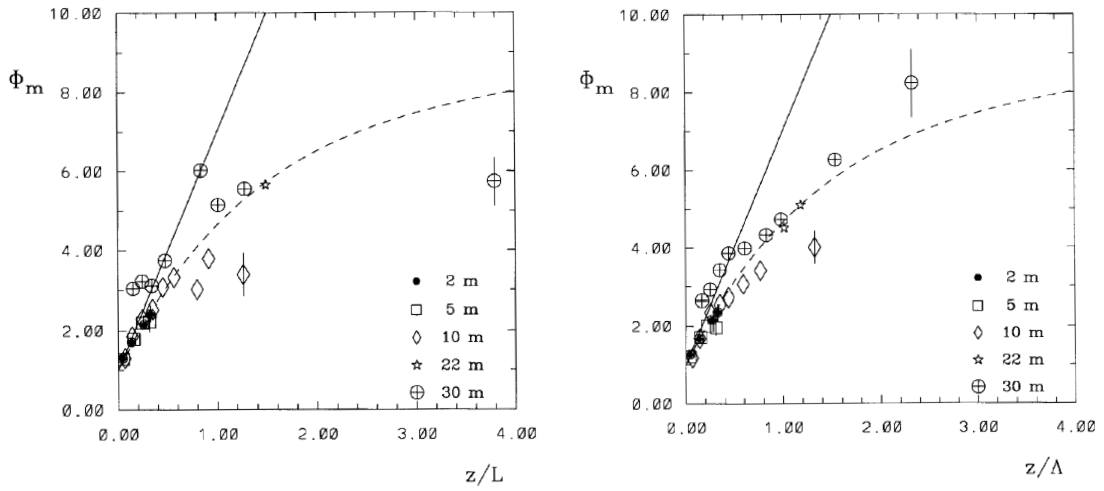

Figure 4.6 Non-dimensional wind shear for stable conditions. Different symbols refer to *average* values for bins of stability from different measurement heights (which should all fall onto the same line according to scaling principles). Vertical bars denote the standard deviation off individual data. The solid line corresponds to Eq. (4.23) with $\beta = 6$ and the dashed line to Eq. (4.24). Left panel: SL scaling, right panel: LS. From Forrer and Rotach (1997).

In order to make this concept useful we therefore secondly need profiles of the turbulent fluxes. These may be obtained simply from observations or, theoretically, under quite stringent conditions: horizontally homogeneous, quasi stationary, with a constant cooling rate and the closure assumption[11] $Ri = R_f = const. = 0.2$. For these conditions, Nieuwstadt (1984) derived

$$\tau / \tau_o = (1 - z/h)^{3/2}$$

$$\overline{w'\theta'} / \overline{w'\theta'}_o = (1 - z/h). \qquad (4.30)$$

In Fig. 1.11 data from the Greenland ice sheet (where at least horizontal homogeneity and the 'constant' cooling rate are no serious problems) are shown to follow this prediction on average.

[11] 'Closures' will be discussed in Chapter 5. Ri and R_f are the *Gradient* and *Flux Richardson* Numbers, respectively, and will be introduced in Chapter 6.

For large values of z/Λ the weak (since suppressed) turbulence will no longer allow for an efficient exchange and the dependence on z is expected to disappear due to the turbulence no longer being able to maintain the exchange with the surface. In terms of *Local Scaling* this means that the scaled variables will approach a constant value for large z/Λ (Nieuwstadt, 1984, Grachev et al. 2013) and the corresponding region is called *z-less scaling* (see Fig. 4.4b). Variables, for which their non-dimensionalization does not contain the height (e.g., the standard deviation of a velocity component) therefore cease to vary with z/Λ (Figure 4.7), while for non-dimensional gradients (where the height is used to non-dimensionalize, see eq. (4.14)) this leads to a linear stability dependence (e.g., $\phi_m = \beta z/\Lambda$, see eq. (4.23), Grachev et al. 2013). This suggests that the form (4.23) for the non-dimensional velocity gradient is consistent with z-less scaling. Babic et al. (2016) find that departure from z-less scaling (and hence linear dependence of ϕ_m on z/Λ) is associated with small-scale turbulence, which in turn is found for Flux Richardson numbers $R_f > 0.25$ (see Chapter 6 for a definition of R_f.

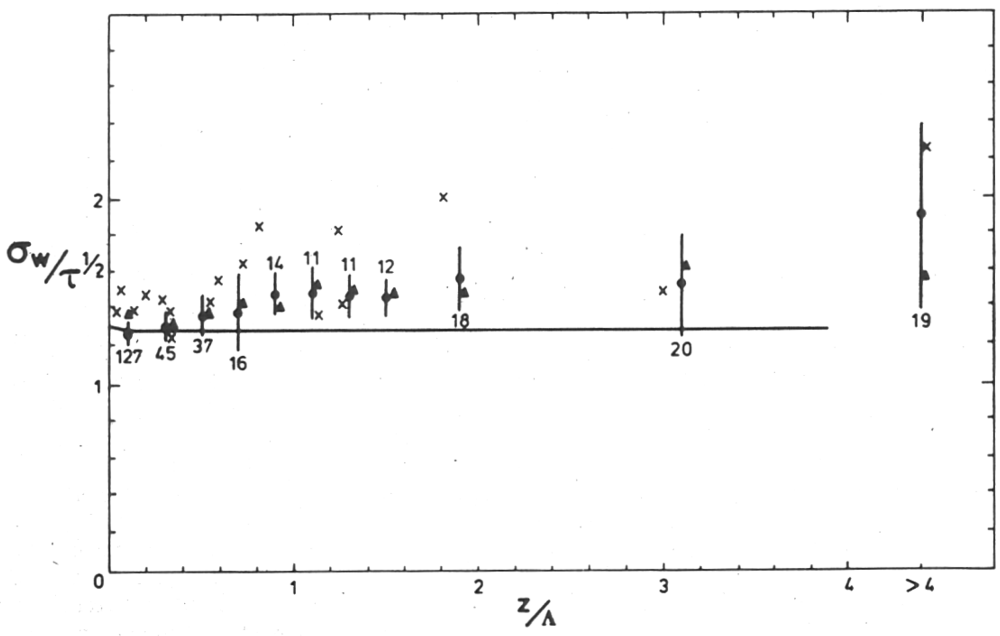

Fig 4.7 Local scaling prediction (solid line) and observations for σ_w/u_* under stable conditions. From Nieuwstadt (1984).

4.5.3 Mixed Layer scaling

Above the SL on the unstable side, Fig. 4.4a reveals the existence of another 'successful' scaling regime, the Mixed Layer (ML). A formal treatment as in Section 4.3 would use the surface heat flux $\overline{w'\theta'}_o$, the height of the layer itself (the so-called mixed layer height z_i), the buoyancy parameter $g/\bar{\theta}$ and the height z as variables to find the non-dimensional height z/z_i as the one and

only 'π-group'. Hence, every carefully scaled variable in the ML is expected to be a function of z/z_i alone (see the synthetic example in Fig. 4.1). This scaling regime originally goes back to the work of Deardorff (1970) among others. For a scaling velocity dimensional analysis yields

$$w_* = (\frac{g}{\overline{\theta}} \overline{w'\theta'}_o z_i)^{1/3}, \tag{4.31}$$

the so-called *convective velocity scale*.

While the ML leads – due to strong turbulence and hence mixing – to essentially vanishing vertical gradients in mean variables (see Fig. 1.5 as an example) it exhibits *characteristic profiles* (dependence on z/z_i) for higher order moments. Figure 1.6 shows typical profiles of the sensible heat flux with the close to linear behaviour from the surface up to the Entrainment Layer. The characteristic profile of the skewness of the vertical velocity component in the ML is depicted in Fig. 4.8. The third order moment is not only different from zero due to strong thermals and compensating subsidence (see Fig. 1.8 and discussion there), but also the skewness is found to be strongly height dependent following the ML scaling prediction. Similar behaviour can be found for many higher order moments in the ML (see Caughey, 1982).

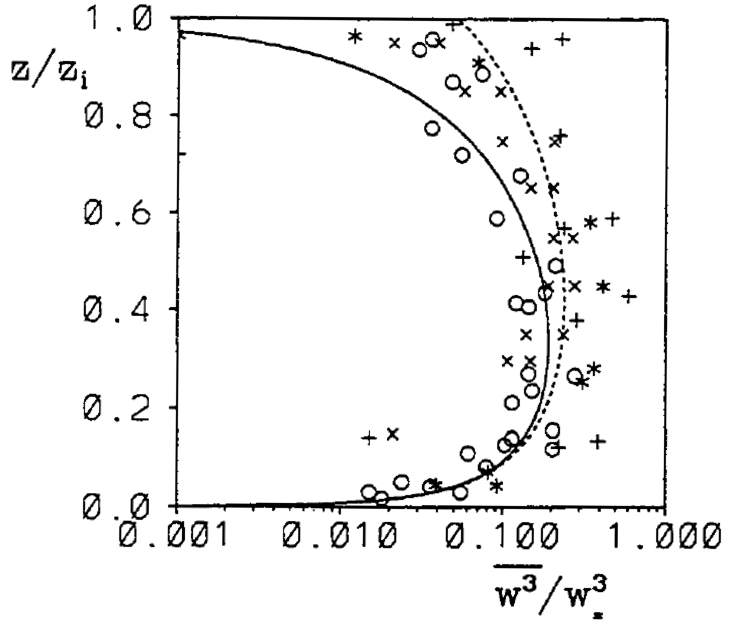

Figure 4.8 ML scaling for the skewness of the vertical velocity component. Data from different full-scale and water tank experiments (different symbols). From Rotach et al. (1996). The solid and dashed line represent two different analytical formulations.

References Chapter 4

Babić K, Rotach MW, Klaić ZB: 2016 Evaluation of Local Similarity Theory in the Wintertime Nocturnal Boundary Layer over Heterogeneous Surface, *Agr Forest Meteorol*, **228**, 164-179. doi: 10.1016/j.agrformet.2016.07.002

Beljaars ACM and Holtslag AAM: 1991, Flux Parameterization Over Land Surfaces for Atmospheric Models, *J Appl Meteorol,* **30**, 327–341.

Beljaars ACM, Bosveld FC: 1997, Cabauw data for the validation of land surface parametrization schemes, *J Clim*, **10**, 1172–1193

Businger JA, Wyngaard JC, Izumi T and Bradley EF: 1971, Flux-profile relationships in the atmospheric surface layer, *J Atm Sci*, **28**, 181-189.

Calanca P: 2001, A note on the roughness length for temperature over melting snow and ice, *Quart J Roy Meteorol Soc*, **127**, 255-260.

Caughey SJ: 1982, Observed characteristics in the atmospheric boundary layer, in: Nieuwstadt FTM and van Dop H (Eds.): Atmospheric turbulence and air pollution modeling, D. Reidel Publ Co, Dordrecht, pp 107-158.

Deardorff JW: 1970, Convective velocity and temperature scales for the unstable planetary boundary layer and for Rayleigh convection, *J Atm Sci*, **27**, 1211-1213.

Forrer J and Rotach MW: 1997, On the Turbulence Structure in the Stable Boundary Layer over the Greenland Ice Sheet, *Boundary-Layer Meteorol.*, **85**, 111-136.

Grachev AA, Andreas EL, Fairall CW, Guest PS, Persson POG: 2013, The Critical Richardson Number and Limits of Applicability of Local Similarity Theory in the Stable Boundary Layer, *Boundary-Layer Meteorol.*, **147**,51–82, DOI 10.1007/s10546-012-9771-0

Högström U: 1988, Non-Dimensional Wind and Temperature Profiles in the Atmospheric Surface Layer: A Re-Evaluation, *Boundary-Layer Meteorol.* **42**, 55–78.

Holtslag, AAM and Nieuwstadt, FTM: 1986, Scaling the Atmospheric Boundary Layer, *Boundary-Layer Meteorol,* **36**, 201-209.

Malhi Y: 1996, The behaviour of the roughness length for temperature over heterogeneous surfaces, *Quart J Roy Meteorol Soc,* **122**, 1095-1125

Monin A and Obukhov AM: 1954, Basic laws of turbulent mixing in the ground layer of the atmosphere, *Tr Akad Nauk SSSR,* **151**, 163-187.

Nieuwstadt FTM: 1984, The turbulent structure of the stable nocturnal boundary layer, *J Atm Sci*, **41,** 2202-2216.

Obukhov, AM: 1946, Turbulence in an Atmosphere with a Non-Uniform Temperature, *Tr Akad Nauk SSSR Inst Teorel Geofis, No 1* (translation in *Boundary-Layer Meteorol*, **2**, 7-29, 1971).

Paulson CA: 1970, The mathematical representation of wind speed and temperature in the unstable atmospheric surface layer. J. Appl. Meteor., 9, 857-861.

Rotach MW, Gryning S-E and Tassone C: 1996, 'A Two-Dimensional Stochastic Lagrangian Dispersion Model for Daytime Conditions', *Quart J Roy Meteorol Soc*, **122**, 367-389.

Sfyri E, Rotach MW, Stiperski I, Bosveld FC, Obleitner F, Lehner M: 2017, Scalar flux similarity in the layer near the surface over mountainous terrain, in review, *Boundary-Layer Meteorol,*

Stull RB: 1988, An introduction to Boundary Layer Meteorology, Kluwer, Dordrecht, 666pp.

Sun J: 1999, Diurnal variations of the thermal roughness length over a grassland, *Boundary-Layer Meteorol,* **92**, 407–427.

Tampieri F, Maurizi A, Viola A: 2009, An Investigation on Temperature Variance Scaling in the Atmospheric Surface Layer, *Boundary-Layer Meteorol*, **132**, 31–42, DOI 10.1007/s10546-009-9383-5

Tillman JE: 1972, The Indirect Determination of Stability, Heat and Momentum Fluxes in the Atmospheric Boundary Layer from Simple Scalar Variables during dry Unstable Conditions, *J Appl Meteorol*, **11** 783-792.

Verma 1989: Aerodynamic resistances to transfers of heat, mass and momentum, in: Black TA, Spittlehouse DL, Novak MD, Price, DT (Eds): Estimation of Areal Evapotranspiration, *Proceedings* of a workshop held at Vancouver, August 1987, IAHS Publ. **177**, 13-20.

Wyngaard JC: 2010, Turbulence in the Atmosphere, Cambridge University Press, 393pp